A Single Methionine Residue Dictates the Kinetic Mechanism of Interprotein Electron Transfer from Methylamine Dehydrogenase to Amicyanin[†,‡]

John K. Ma,[§] Yongting Wang,[§,⊥] Christopher J. Carrell,[∥] F. Scott Mathews,[∥] and Victor L. Davidson*[,§]

Department of Biochemistry, The University of Mississippi Medical Center, Jackson, Mississippi 39216-4505, and Department of Biochemistry and Molecular Biophysics, Washington University School of Medicine, St. Louis, Missouri 63110

Received June 21, 2007; Revised Manuscript Received July 24, 2007

ABSTRACT: Amicyanin is a type 1 copper protein that is the natural electron acceptor for the quinoprotein methylamine dehydrogenase (MADH). A P52G amicyanin mutation increased the K_d for complex formation and caused the normally true electron transfer (ET) reaction from *O*-quinol MADH to amicyanin to become a gated ET reaction (Ma, J. K., Carrell, C. J., Mathews, F. S., and Davidson, V. L. (2006) *Biochemistry 45,* 8284−8293). One consequence of the P52G mutation was to reposition the side chain of Met51, which is present at the MADH−amicyanin interface. To examine the precise role of Met51 in this interprotein ET reaction, Met51 was converted to Ala, Lys, and Leu. The K_d for complex formation of M51A amicyanin was unchanged but the experimentally determined electronic coupling increased from 12 cm^{-1} to 142 cm^{-1}, and the reorganization energy increased from 2.3 to 3.1 eV. The rate and salt dependence of the proton transfer-gated ET reaction from *N*-quinol MADH to amicyanin is also changed by the M51A mutation. These changes in ET parameters and rates for the reactions with M51A amicyanin were similar to those caused by the P52G mutation and indicated that the ET reaction had become gated by a similar process, most likely a conformational rearrangement of the protein ET complex. The results of the M51K and M51L mutations also have consequences on the kinetic mechanism of regulation of the interprotein ET with effects that are intermediate between what is observed for the reaction of the native amicyanin and M51A amicyanin. These data indicate that the loss of the interactions involving Pro52 were primarily responsible for the change in K_d for P52G amicyanin, while the interactions involving the Met51 side chain are entirely responsible for the change in ET parameters and conversion of the true ET reaction of native amicyanin into a conformationally gated ET reaction.

Long-range electron transfer (ET)[1] between proteins is a process that is fundamental to respiration, photosynthesis, and redox reactions of intermediary metabolism. Many physiological long-range biological ET reactions are bimolecular processes involving donor and acceptor proteins. The overall redox reaction may require several steps, including specific binding of proteins, protein rearrangements that optimize the coupling between redox centers, chemical transformations such as proton transfer, and the actual ET step. Such interprotein ET reactions may be classified according to the nature of the rate-limiting step for the overall reaction (*1*, *2*). If the actual ET step is rate limiting for the overall process, the overall reaction is considered a true ET reaction. Alternatively, if another reaction step that precedes ET is completely rate limiting so that the observed rate is actually that of a non-ET event, then the overall reaction is considered gated ET (*3*, *4*). It is also possible that a reaction step that precedes ET is rapid relative to ET but very unfavorable so that the observed rate is influenced by the equilibrium constant for that non-ET process. This is considered kinetically coupled ET (*5*−*7*).

Methylamine dehydrogenase (MADH) (*8*), amicyanin (*9*), and cytochrome *c*-551i (*10*) from *Paracoccus denitrificans* form one of the best characterized physiological ET complexes of proteins. X-ray crystal structures are available for the binary complex of MADH (*11*) and amicyanin, and for a ternary protein complex (*12*), which includes cytochrome *c*-551i, the electron acceptor for amicyanin. It was demonstrated by single-crystal polarized absorption microspectroscopy (*13*) and EPR spectroscopy (*14*) that in the crystalline state, these complexes can catalyze the oxidation of methylamine and subsequent ET from MADH to amicyanin and from amicyanin to the cytochrome. ET between the tryptophan tryptophylquinone (TTQ) (*15*) prosthetic group of MADH and the type 1 copper center of amicyanin has been studied in solution in the steady state (*16*) and by stopped-flow spectroscopy (*17*−*20*). It is possible to study ET from

[†] This work was supported by NIH Grant GM-41574 (to V.L.D.) and NSF Grant MCB0343374 (to F.S.M.).

[‡] Crystallographic coordinates have been deposited in the Protein Data Bank under the file names 2QDV for Cu(II) M51A and 2QDW for Cu(I) M51A amicyanins.

* Corresponding author. Department of Biochemistry, University of Mississippi Medical Center, 2500 N. State St., Jackson, Mississippi 39216-4505. Tel: 601-984-1516. Fax: 601-984-1501. E-mail: vdavidson@biochem.umsmed.edu.

[§] The University of Mississippi Medical Center.

[∥] Washington University School of Medicine.

[⊥] Present address: Department of Biology, Massachusetts Institute of Technology, Cambridge, MA 02139.

[1] Abbreviations: MADH, methylamine dehydrogenase; TTQ, tryptophan tryptophylquinone; ET, electron transfer; H_{AB}, electronic coupling; λ, reorganization energy; E_m, oxidation−reduction midpoint potential; PT, proton transfer; DSC, differential scanning calorimetry; rmsd, root mean square difference.

10.1021/bi7012307 CCC: $37.00
Published on Web 09/08/2007

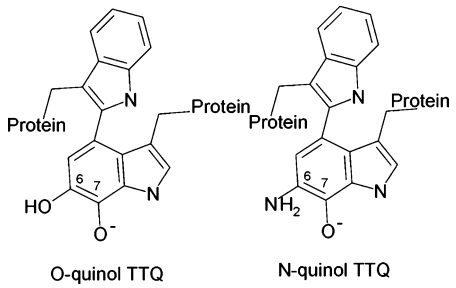

FIGURE 1: Different forms of reduced TTQ in methylamine dehydrogenase. Chemical reduction of MADH by dithionite yields the *O*-quinol form of TTQ. Reduction of MADH by the amine substrate yields an *N*-quinol form of TTQ in which the substrate-derived nitrogen has displaced the oxygen at the C6 position.

different reduced forms of MADH to amicyanin (Figure 1) (*21*). The product of the reduction of MADH by the substrate amine is an *N*-quinol, which retains the covalently bound substrate-derived amino group after release of the aldehyde product. An *O*-quinol form of MADH may be generated by reduction by dithionite. The reaction of *O*-quinol MADH with amicyanin is a true ET reaction (*17*−*19*), which yields values of reorganization energy (λ) of 2.3 eV, electronic coupling (H_{AB}) of 12 cm^{-1}, and a predicted ET distance that approximates that seen in the crystal structure. The values of the ET parameters were determined from the temperature dependence (*17*) and the ΔG^o dependence (*18*, *19*) of the redox reaction. In contrast, under physiological conditions ET from *N*-quinol MADH to amicyanin is a chemically gated reaction (*4*), which yields unreasonable values of λ of 3.5 eV and H_{AB} of 23,000 cm^{-1} (*20*). It was subsequently shown that the observed rate of this reaction is that of the deprotonation of the *N*-quinol amino group, which is dependent on the presence of a monovalent cation (*22*, *23*).

The copper center of oxidized amicyanin possesses four coordinating ligands: two N^{δ} of His95 and His53, sulfur of Cys92, and sulfur of Met98 at a longer distance forming a distorted tetrahedral geometry (*24*). We have previously shown that mutation of residues near the copper center and its ligands affects the ET reactions from TTQ to copper in a variety of ways. P94F and P94A mutations of amicyanin significantly increase the E_m value of copper, thus increasing ΔG^o for the true ET reaction, which results in an increase in the ET rate constant (k_{ET}) (*25*, *26*). An F97E mutation decreases the H_{AB} for the true ET reaction by perturbing the protein−protein interface, thus decreasing k_{ET} (*27*). A P52G mutation altered the observed rate for the ET transfer from TTQ to copper by changing the rate-limiting step in the overall redox reaction such that the true ET reaction was converted to one which was conformationally gated (*28*). It was concluded that the P52G mutation altered the positions of residues involved in protein−protein interactions within the ET protein complex such that a rate-limiting conformational rearrangement of proteins within the complex was required to poise the system for the true ET event. In addition to the loss of three carbons of Pro52 in P52G amicyanin, it was noted the P52G mutation resulted in a change in position of the side chain of Met51, which eliminated the contacts with the side chain of βVal58 of MADH that are seen in the structure of the complex of native amicyanin with MADH (*28*).

In this article, Met51 was mutated to alanine to mimic the loss of interactions involving the Met51 side chain that was observed in P52G amicyanin so that the significance of this residue in determining the kinetic regulation of the interprotein ET reaction could be determined independent of the change Pro52. Met51 was also mutated to lysine and leucine to provide further insight into the mechanism of this regulation. The results indicate that the conformational gating of the ET reaction that was caused by the P52G mutation may be attributed completely to the loss of interprotein interactions involving the side chain of Met51. The hydrophobic interactions of that single residue with MADH at the protein−protein interface dictate the kinetic mechanism of this interprotein ET reaction.

EXPERIMENTAL PROCEDURES

Protein Preparation. MADH (*29*) and amicyanin (*9*) were purified from *P. denitrificans* as previously described. Protein concentrations were calculated from known extinction coefficients of oxidized amicyanin (ϵ_{595} = 4610 cm^{-1} M^{-1}) and oxidized MADH (ϵ_{440} = 26,200 cm^{-1} M^{-1}). *O*-quinol MADH and reduced amicyanin were generated by titration of the oxidized proteins with stoichiometric amounts of dithionite. *N*-quinol MADH is formed by stoichiometric reduction by methylamine.

Protein Expression. Site-directed mutagenesis to create M51A, M51K, and M51L amicyanins were performed on double stranded pMEG201 (*30*), which contains the gene *mauC* (*31*) that encodes amicyanin, using mutagenic primers with QuikChange Site-Directed Mutagenesis Kit (Stratagene). The oligonucleotide sequences used to construct the M51A mutant were 5′-CGCGAGGCGGCGCCGCACAATGTC-CATTTCG -3′ and its complementary DNA; for the M51K mutant, 5′-CGCGAGGCGAAGCCGCACAATGTC-CATTTCG -3′ and its complementary DNA; and for the M51L mutant, 5′-CGCGAGGCGCTGCCGCACAATGTC-CATTTCG -3′ and its complementary DNA. The underlined bases are those that were changed to create the desired change in the amino acid sequence and to generate a new restriction site that was used to facilitate screening. The entire 555-base *mau*C-containing fragment was sequenced to ensure that no second site mutations were present, and none were found. The mutant amicyanins were expressed in *E. coli* and purified from the periplasmic fraction as described for other recombinant amicyanin mutants (*30*).

Spectrochemical Redox Potential Determination. The E_m values of M51A, M51L, and M51K amicyanins were determined by spectrochemical titration as described previously for native amicyanin (*32*). The ambient potential was measured directly with a Corning combination redox electrode, which was calibrated using quinhydrone (a 1:1 mixture of hydroquinone and benzoquinone) as a standard with an E_m value of +286 mV at pH 7.0 (*33*). The reaction mixture contained 340 μM amicyanin in 0.05 M BisTris propane (BTP) buffer at the indicated pH, at 25 °C. Ferricyanide (1 mM) and quinhydrone (200 μM) were used as mediators, and the mixture was titrated by addition of incremental amounts of ascorbate, which was used as a reductant. In the oxidative direction, titration by addition of potassium ferricyanide was performed. The absorption spectrum of amicyanin was recorded at different ambient potentials (*E*), and

Table 1: Data Collection and Refinement Statistics

sample	M51A Cu(II)	M51A Cu(I)
data collection		
wavelength (Å)	0.9000	0.9000
space group	$P2_1$	$P2_1$
a (Å)	28.36	28.21
b (Å)	55.39	55.36
c (Å)	27.01	27.27
β (°)	94.82	95.75
max. resolution (outer shell) (Å)	0.89 (0.91−0.89)	0.92 (0.94−0.92)
$I/\sigma(I)$[a]	27.2 (7.7)	12.0 (4.8)
no. of observations	207933	382587
no. unique reflections	52990	53675
percent completion (outer shell)	83.3 (41.2)	92.2 (45.3)
redundancy	3.9 (3.4)	7.1 (3.2)
R_{merge}[b] (outer shell)	0.040 (0.183)	0.081 (0.259)
refinement		
data range (Å)	30−0.89	30−0.92
no. of reflections/free set	50307/2671	39881/2117
R_{work}[c]	0.110	0.108
R_{free}[c]	0.135	0.148
R_{total}[c]	0.111	0.111
no. protein atoms	829	817
no. copper ions	1	2
no. solvent molecules	196	163
no. other atoms	5	10
$\langle B\rangle$ protein atoms (Å^2)[d]	8.3	10.6
$\langle B\rangle$ anion atoms (Å^2)[d]	31.2	25.2
$\langle B\rangle$ solvent atoms (Å^2)[d]	21.9	27.3
rms ΔB (m/m, Å^2)[d,e]	1.4	1.7
rms ΔB (m/s, Å^2)[d,e]	1.9	3.0
rms ΔB (s/s, Å^2)[d,e]	3.9	4.9

[a] $I/\sigma(I)$ is the average signal-to-noise ratio for merged reflection intensities. [b] $R_{merge} = \Sigma_h\Sigma_I |I(h) - I_i(h)|/\Sigma_h\Sigma_i I_i(h)$, where $I_i(h)$ is the *i*th measurement, and $I(h)$ are the mean measurements of reflection *h*. [c] $R = \Sigma_h |F_o - F_c|/\Sigma_h |F_o|$, where F_o and F_c are the observed and calculated structure factor amplitudes, respectively, of reflection *h*. R_{free} is *R* for the test reflection data set (5% of the observed reflections) for cross validation of the refinement (*45*), R_{work} is *R* for the working reflection set, and R_{total} is *R* for all the data. [d] The *B*-values shown refer to the isotropic equivalent of the anisotropic thermal parameters used during the refinement. [e] Root-mean-square difference in *B*-factor for bonded atoms; m/m, m/s, and s/s represent main chain−main chain, main chain−side chain, and side chain−side chain bonds, respectively.

the concentrations of oxidized amicyanin and reduced amicyanin were determined by comparison with the spectra of the completely oxidized and reduced forms. E_m was determined from the fit of the data to eq 1.

$$E = E_m + 2.3RT/nF \log [\text{amicyanin}]_{ox}/[\text{amicyanin}]_{red} \quad (1)$$

Electron Paramagnetic Resonance Spectroscopy. X-band EPR spectra were recorded on a Bruker EMX spectrometer equipped with an ESR910 liquid helium cryostat at 20 K with a frequency of 9.38388 GHz, power of 0.2 mW, and modulation frequency of 100 kHz. The sample contained 200 μM of M51A, M51K, or M51L amicyanin in 5% glycerol and 10 mM potassium phosphate at pH 7.4.

Differential Scanning Calorimetry. Solution DSC was performed, and data was analyzed as described previously for native amicyanin (*34*) with a Calorimetry Sciences Corporation 6100 Nano II DSC with tantalum cells with a nominal volume of 0.33 mL. The buffer and the sample were scanned from 25 to 100 °C. As was reported for native amicyanin, it was not possible to obtain ΔH values for the calorimetric enthalpy of unfolding because of the irreversibility of the thermal denaturation, but it was possible to accurately determine T_m values, which define the midpoint temperature for the thermal transition.

Electron Transfer Reactions. An On-Line Instruments (OLIS, Bogard, GA) RSM rapid scanning stopped-flow spectrophotometer was used for kinetic measurements. Experiments were performed in 0.01 M potassium phosphate buffer at pH 7.5. The experimental details and methods of data analysis have been previously described (*35*). To study the ET reaction from MADH to amicyanin, prior to mixing one syringe contained either 2 μM reduced *O*-quinol or 2 μM *N*-quinol MADH, while the other contained varying concentrations of oxidized amicyanin. Pseudo-first-order conditions were maintained with excess amicyanin to MADH. ET reactions were fit to the simple kinetic model in eq 2 using eq 3 where A and B are the contents of the mixing syringes described above.

$$A_{ox} + B_{red} \overset{K_d}{\rightleftharpoons} A_{ox}/B_{red} \overset{k_3}{\underset{k_4}{\rightleftharpoons}} A_{red}/B_{ox} \quad (2)$$

$$k_{obs} = k_3 [\text{amicyanin}]/(K_d + [\text{amicyanin}]) + k_4 \quad (3)$$

Analysis of the Temperature Dependence of Reaction Rates. The temperature dependence of k_3 was analyzed according to ET theory (*36*) (eqs 4 and 5). H_{AB} is the electronic coupling constant, λ is the reorganization energy, *h* is Plank's constant, *T* is temperature, *R* is the gas constant, and k_o is the characteristic frequency of nuclei (10^{13} s^{-1}), which is the maximum ET rate when donor and acceptor are in van der Waals contact and $\lambda = -\Delta G^o$. The donor to acceptor distance is *r*, and r_o is the close contact distance (3 Å). β is used to quantitate the nature of the intervening medium with respect to its efficiency to mediate ET. ΔG^o is determined from the ΔE_m value for the reaction from eq 6.

$$k_{ET} = \frac{4\pi^2 H_{AB}^{\ 2}}{h\sqrt{4\pi\lambda RT}} e^{-(\Delta G^0+\lambda)^2/4\lambda RT} \quad (4)$$

$$k_{ET} = k_o \exp[-\beta(r - r_o)]\exp[-\Delta G^o + \lambda)^2/4\lambda RT) \quad (5)$$

$$\Delta G^o = -nF\Delta E_m \quad (6)$$

X-ray Structure Determination. Crystals of M51A amicyanin were grown by macroseeding using a 9-to-1 mixture of monobasic sodium (3 M) and dibasic potassium (3 M) phosphate solutions as precipitant as described previously (*37*). The crystals are monoclinic, space group $P2_1$, contain one molecule per asymmetric unit, and are isomorphous with crystals of the native protein. Cell dimensions are given in Table 1. X-ray diffraction data from a dark blue oxidized M51A amicyanin crystal and a colorless reduced protein crystal were recorded at the BIOCARS beamline 14-BM-C with an ADSC-Q4 CCD detector; for crystal reduction, the crystal was incubated for about 30 min in a solution of 10 mM sodium ascorbate in 4 M monobasic sodium/dibasic potassium phosphate buffer in the ratio 4:1 (pH ~5.5) prior to data collection. For both crystals, the data were recorded at 100 K, using paratone-N oil (Hampton Research, Laguna Hills, CA) as a cryoprotectant, to 0.89 Å and 0.92 Å resolution, respectively. The data from the oxidized crystal were collected approximately 1 week after crystallization and from the reduced crystal approximately 1 month after growth of the crystal. Both data sets were processed using DENZO

Table 2: Physical Properties of Native and Met51 Mutant Amicyanins

property	native amicyanin	M51A amicyanin	M51K amicyanin	M51L amicyanin
absorption λ_{max} (nm)	595	595	595	595
EPR $-$ g_{II}	2.239	2.247	2.243	2.256
EPR $-$ A_{II} (G)	53	62	56	54
T_m oxidized (°C)	67.7 ± 0.1[a]	66.4 ± 0.1	61.8 ± 0.31	64.2 ± 0.1
T_m reduced (°C)	62.4 ± 0.1[a]	63.6 ± 0.1	63.8 ± 0.1	63.3 ± 0.1
E_m pH 7.4 (mV)	266 ± 7[b]	256 ± 1	267 ± 1	257 ± 1
E_m pH 9.0 (mV)	240 ± 7[b]	232 ± 1	242 ± 1	245 ± 1

[a] Ref *34*. [b] Ref *32*.

and SCALEPACK (*38*). The data collection statistics are presented in Table 1.

The structures of both forms of M51A amicyanin were refined directly from the oxidized wild-type protein structure determined at 0.75 Å resolution (PDB ID 2OV0; unpublished results) after prior removal of solvent molecules and alternate amino acid conformations using SHELX (*39*). Alternating cycles of refinement and model building in XtalView were carried out. Hydrogen atoms, positioned as a riding model, were included in the refinements in SHELX. The temperature factors of all non-hydrogen atoms were refined anisotropically. The refinement statistics can be found in Table 1.

Modeling and Surface Area Calculations. Structural comparisons of Cα positions were carried out using LSQMAN (*40*). In comparing mutant and native amicyanin structures, residues 1−21 were omitted from the calculations since they are known to be quite flexible, and only the remaining, relatively rigid, 85 residue C-terminal portions of the structures were retained.

RESULTS

Physical Properties of M51A, M51L, and M51K Amicyanins. Despite the pronounced effects of the mutations of residue Met51 on the ET reaction from MADH to amicyanin (discussed later), the physical properties of M51A, M51L, and M51K amicyanins are very similar to those of native amicyanin (Table 2). The visible absorption spectrum of oxidized M51A, M51L, and M51K amicyanins are essentially identical to that of native amicyanin and exhibit a broad peak centered at 595 nm with an extinction coefficient of about 4600 cm^{-1} M^{-1}. The EPR spectra of oxidized native, M51A, M51L, and M51K amicyanins exhibit similar values of g_{II} and hyperfine splitting A_{II}, which are typical of a type 1 copper site with axial symmetry characterized by four hyperfine lines. We have previously studied the stability of native amicyanin using solution DSC and demonstrated that the major thermal transition that occurs in the DSC profile correlates with disruption of the type 1 copper geometry (*34*). The T_m values for the major transitions of the oxidized and reduced M51A, M51L, and M51K amicyanins at pH 7.5 are very similar to the respective values obtained previously for oxidized and reduced native amicyanin. The E_m values determined for M51A, M51L, and M51K amicyanins in solution at pH 7.4 and pH 9 are very similar to those of native amicyanin. We previously showed that the E_m value of native amicyanin is pH dependent with a pK_a value of 7.7 because reduced amicyanin exhibits a pH-dependent conformational change in which the His95 copper ligand rotates out of the coordination sphere of the reduced copper when protonated (*32*). These results indicate that the mutations of residue Met51 had no significant effect on either the magnitude or the pH dependence of the E_m value.

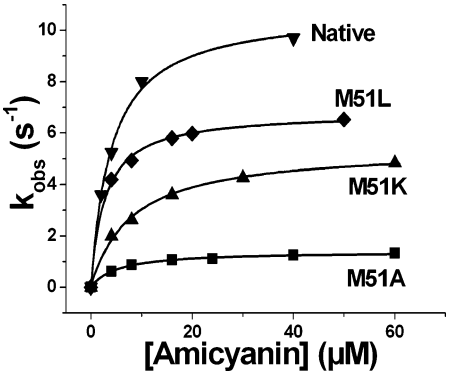

FIGURE 2: Dependence of the rate of the ET reaction from *O*-quinol MADH on amicyanin concentration. Native amicyanin (▼), M51A amicyanin (■), M51K amicyanin (▲), and M51L amicyanin (♦). The solid lines represent fits of the data to eq 3.

ET from O-Quinol MADH to M51A, M51L, and M51K Amicyanins. The ET reactions from *O*-quinol MADH to each of the Met51 mutant amicyanins each exhibited a hyperbolic dependence of k_{obs} on amicyanin concentration (Figure 2). As such, it was possible to determine values of K_d and the limiting first-order rate constant for the redox reaction (k_3 in eq 2). The ET reaction from *O*-quinol MADH to oxidized native amicyanin is a true ET reaction (*17*−*19*). On the basis of the $\Delta G°$ values determined from ΔE_m, if ET from *O*-quinol MADH to M51A amicyanin were also a true ET reaction, then k_{ET} should be only slightly less than that observed for the reaction with native amicyanin. Instead, the k_3 value determined at 30 °C is about 8-fold less than that of the native reaction (Table 3). Interestingly, this rate is much more similar to the rate previously determined for the reaction with P52G amicyanin, which is not a true ET reaction but one which is conformationally gated (*28*). In contrast to the k_3 values, the K_d value determined for complex formation between *O*-quinol MADH and M51A amicyanin is similar to that of the native amicyanin and much lower than for P52G amicyanin (Table 3). The rates of ET from *O*-quinol MADH to M51K and M51L amicyanins are intermediate between that of M51A amicyanin and native amicyanin.

The k_3 values for the ET reaction from *O*-quinol MADH to each oxidized amicyanin were determined over a range of temperatures from 15 to 44 °C, and the data were analyzed using eqs 4 and 5 (Figure 3 and Table 3). The values of λ, H_{AB}, and r determined for the ET reactions from *O*-quinol MADH to M51A and M51K amicyanins were significantly different from those that describe the reaction with native amicyanin but were similar to the parameters that describe the gated ET reaction from *O*-quinol MADH to P52G amicyanin. In particular, the values of H_{AB} for the reactions of M51A and M51K amicyanins appear to exceed the nonadiabatic limit, often taken to be <80 cm^{-1} (*41*). The corresponding fitted values of r are also unreasonably small given the known structure of the complex. These observations as well as the large increase in values of λ for these two reactions all indicate that the M51A and M51K mutations have caused a change in the kinetic mechanism of regulation of the ET reaction such that the reactions with M51A and

Table 3: Electron Transfer Parameters for the Reactions of *O*-quinol MADH with Native and Mutant Amicyanins

parameters	native amicyanin[a]	P52G amicyanin[b]	M51A amicyanin	M51K amicyanin	M51L amicyanin
K_d (μM)	4.5	38	6.8	11	6.8
k_3, 30 °C (s^{-1})	10	3.0	1.3	4.9	6.8
ΔG^o (kJ mol^{-1})	−3.18	−4.82	−2.84	−3.37	−3.66
λ (kJ mol^{-1})[c]	222 ± 10	270 ± 10	296 ± 3	290 ± 4	246 ± 10
λ (eV)	2.30 ± 0.1	2.8 ± 0.1	3.07 ± 0.03	3.0 ± 0.04	2.55 ± 0.1
H_{AB} (cm^{-1})	12 ± 7	78 ± 30	142 ± 20	194 ± 40	23.3 ± 10
r (Å) $\beta = 1.0$ $Å^{-1}$	9.5 ± 0.8	6 ± 0.9	4.7 ± 0.3	4.1 ± 1	8.3 ± 0.4

[a] Taken from ref *17*. In that reference, a range of values of ΔG^o was used to yield a range of values of λ because at that time it was uncertain as to whether it was most appropriate to use the E_m value of free amicyanin or amicyanin in complex with MADH. The data in this table were recalculated using what is now known to be the appropriate ΔG^o as well as a β value of 1.0 $Å^{-1}$, which is generally accepted as reasonable for protein β sheets (*46*) to fit for r. [b] Taken from ref *28*. [c] λ is sometimes expressed in units of kJ/mol and sometimes as eV; therefore, both values are given.

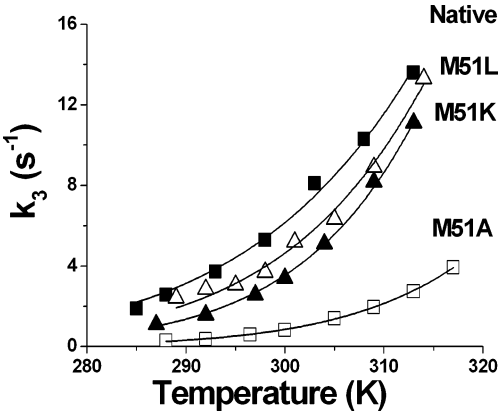

FIGURE 3: Dependence of the rate of the ET reaction from reduced *O*-quinol MADH to amicyanins on temperature. Native amicyanin (■), M51A amicyanin (□), M51K amicyanin (▲), and M51L amicyanin (△). The solid lines represent fits of the data to eq 5.

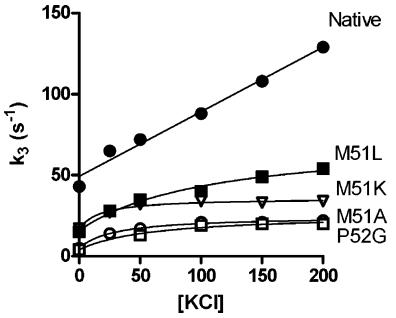

FIGURE 4: Dependence of the rate of the ET reaction from *N*-quinol MADH to mutant amicyanins on [KCl]. The line for native amicyanin (●) is a fit to linear regression. The curves for M51L amicyanin (■), M51K amicyanin (▽), M51A amicyanin (○), and P52G amicyanin (□) are fits to a hyperbolic function. Data for P52G amicyanin is taken from ref *28*.

M51K amicyanins are gated ET reactions. Furthermore, the process that is now rate determining for the overall redox reaction with M51A amicyanin appears to be the same as that which gates the ET reaction with P52G amicyanin (discussed later). The values of λ, H_{AB}, and r determined for the ET reaction from *O*-quinol MADH to M51L amicyanin were intermediate between those determined in the reactions of M51A amicyanin and native amicyanin.

ET from N-Quinol MADH to M51A, M51L, and M51K Amicyanins. The ET reaction from *N*-quinol MADH to amicyanin is not a true ET reaction but one which is chemically gated (*4*) by a rate-limiting deprotonation of the *N*-quinol to generate an activated intermediate from which very rapid ET occurs (*20*, *23*). Thus, this reaction is much faster than the reaction of the *O*-quinol MADH, despite being a gated ET reaction. The limiting first-order rate constant for the chemically gated ET reaction of *N*-quinol amicyanin is sensitive to salt concentration since the rate-limiting proton transfer requires the presence of a monovalent cation at the active site (*23*). It exhibits a linear dependence on [KCl] up to 200 mM. The reactions of *N*-quinol MADH with oxidized M51A, M51L, and M51K amicyanins were also salt dependent (Figure 4) but to a different extent than the reaction with native amicyanin. The rate of the reaction with M51A amicyanin increases with salt and plateaus at about 100 mM KCl. The observed rates and salt dependence of the reaction with M51A amicyanin are nearly identical to those previously reported for the reaction with P52G amicyanin (*28*) (Figure 4). The rate of the reaction with M51K amicyanin also increases with salt and plateaus at about 100 mM KCl. The rate of the reaction with M51L amicyanin exhibits a gradual hyperbolic increase that has not yet reached a plateau at a 200 mM KCl. It is not possible test higher salt concentrations because this disrupts complex formation between MADH and amicyanin.

Crystal Structure. It was possible to crystallize and obtain the structures of the oxidized and reduced forms of M51A amicyanin refined to 0.89 and 0.90 Å, respectively. Analysis of the structural quality of these crystals using PROCHECK indicates that all the residues are in either the most favored or the additionally allowed regions of the Ramachandran plot (*42*). The oxidized M51A amicyanin structure exhibits alternate conformations for five side chains (Val16, Lys38, Met71, Thr87, and Asp89), while the reduced M51A amicyanin exhibits alternate conformations for three side chains (Met71, Asp89, and His95) plus the copper ion; the latter also binds a phosphate anion. In addition, both structures contain a modified Met28 side chain in which an oxygen atom has been added at the SG position to form a sulfoxide product. In both structures, the residue at this position is in two alternate conformations: one of which (at 55% occupancy in the oxidized and 25% occupancy in the reduced) is the unmodified form of Met28, and the other (at 45% occupancy oxidized, 75% occupancy in the reduced) is the methoxy form of that side chain.

The oxidized and reduced M51A amicyanin structures are very similar to each other, with a rmsd between equivalent Cα atoms of 0.18 Å for all 105 residues. The largest deviation occurs near position Asp18 (0.74 Å), which is located within a very flexible loop segment near the

Table 4: Root-Mean-Square Deviations (rmsd) between Three Aligned Amicyanin Structures[a]

proteins aligned	native amicyanin	P52G amicyanin
M51A amicyanin(Å)	0.25 Å	0.18 Å
P52G amicyanin (Å)	0.13 Å	

[a] The structures used in this comparison were oxidized M51A amicyanin (PDB ID 2QDV), oxidized P52G amicyanin (PDB ID 2GB2), and oxidized native amicyanin (PDB ID 2OV0). Structural alignments were based on the relatively rigid 85-residue C-terminal fragments of each protein with the flexible peptide fragment 1−21 omitted.

Table 5: Root-Mean-Square Deviations (rmsd) between Peptide Segments of Three Aligned Amicyanin Structures[a]

peptide segment[b]	26−28	48−52	73−74	83−86
M51A vs native (Å)	0.74	0.58	0.29	0.30
P52G vs native (Å)	0.31	0.21	0.17	0.22
M51A vs P52G (Å)	0.45	0.43	0.30	0.14

[a] The structures used in this comparison were oxidized M51A amicyanin (PDB ID 2QDV), oxidized P52G amicyanin (PDB ID 2GB2), and oxidized native amicyanin (PDB ID 2OV0). Structural alignments were based on the relatively rigid 85-residue C-terminal fragment with the flexible peptide fragment 1−21 omitted. [b] The peptide segments identified show differences between aligned Cα atoms of 0.20 Å or greater for two or more consecutive residues between M51A and native amicyanins.

N-terminus (residues 1−21) of variable conformation (*25*). When residues 1−21 are omitted from the calculation, the rmsd reduces to 0.15 Å for 84 Cα atoms. Consequently, subsequent amicyanin comparisons are limited to the relatively rigid 84-residue C-terminal portion of the molecule (discussed in Experimental Procedures). Two other segments show discernible differences with two or more residues differing by 0.2 Å or greater, one at Ala51 (0.49 Å) and the other at Pro94 (0.47 Å), which are, respectively, the site of the M51A mutation and the site adjacent to His95, one of the copper ligands. In reduced M51A amicyanin, one conformer of His 95 (at about half occupancy) is coordinated to one of the alternate copper sites (also at about half occupancy), which is also coordinated to the side chains of His53, Cys92, and Met98, similar to the copper coordination in the oxidized M51A amicyanin structure. The other His95 side chain conformer is in a flipped configuration (*32*), unbound to copper and instead hydrogen bonded to water molecules. The corresponding alternate copper site is 3-coordinate, bound to the side chains of His53, Cys92, and Met98 and is located 1.14 Å from the first copper site. This situation is very similar to that observed in the crystal structures of reduced forms of native amicyanin (PDB ID 2RAC) (*32*) as well as other site-directed mutants of amicyanin (*25*, *43*).

When the oxidized M51A, P52G, and native amicyanin structures are compared (Table 4), the native and P52G amicyanin structures are most similar (0.13 Å rmsd), while the M51A and native amicyanin structures are most deviant (0.25 Å rmsd). The differences between the two mutant structures are intermediate (0.18 Å rmsd). In these comparisons, only the relatively rigid 84-residue portions (22−105) have been compared, and only the M51A amicyanin form containing unmodified Met28 was used. On further comparison of the structures (Table 5), there are four segments that show significant deviations between them containing two or more adjacent residues differing by 0.2 Å or greater. These are Ala26−Met28 (0.74 Å rmsd), Arg48−Pro52 (0.58 Å rmsd), Lys73−Lys74 (0.28 Å rmsd), and Thr83−Gly86 (0.30 Å rmsd). Comparison of M51A with P52G amicyanins shows deviations of 0.45, 0.43, and 0.28 Å, respectively, for the first three segments and less than 0.2 Å for the fourth. The comparison of P52G with native amicyanin shows smaller deviations of 0.31, 0.26, and 0.25 for the first, second, and fourth segments and less than 0.2 Å for the third segment.

Only the first three of these segments are within or close to the MADH/amicyanin interface in the native complex. Unfortunately, it has not been possible to obtain crystals of either the M51A and P52G amicyanins in complex with MADH as was done previously with native amicyanin (*11*, *12*). The second segment, Arg48−Pro52, contains the sites of mutation for both M51A and P52G amicyanins and would be expected to differ to a similar extent from native amicyanin for both mutants. However, the difference is considerably larger for M51A amicyanin than for P52G amicyanin and is significant between them. Unexpectedly, the first segment, Ala26−Met28 also differs to a large extent between M51A amicyanin and both native and P52G amicyanins. The third and fourth segments show considerably smaller deviations among the three forms, with the third segment behaving similarly in P52G and native amicyanins, while the fourth segment behaves differently in the native amicyanin compared to the M51A and P52G amicyanin structures.

DISCUSSION

Both hydrophobic and electrostatic forces are important in the interactions between native MADH and amicyanin (*30*). The side chain of αAsp180 of the MADH large subunit forms a salt bridge with Arg99 of amicyanin. It was demonstrated by site-directed mutagenesis of each of these two residues that this salt bridge accounts for the stabilization of the complex at low ionic strength and decreases the K_d for the MADH amicyanin complex at low ionic strength by about 100-fold (*30*, *44*). Hydrophobic residues that have been implicated to play a vital role at the binding interface of MADH and amicyanin include Met71, Met51, Met28, Pro52, Pro94, Pro96, and Phe97 of amicyanin (Figure 5). A significant role of Phe97 in stabilizing the complex was demonstrated by site-directed mutagenesis of this residue (*27*, *30*). It was recently shown that a P52G mutation altered the positions of residues 52 and 51, which are both involved in protein−protein interactions within the ET protein complex, such that a rate-limiting conformational rearrangement of proteins within the complex was required to poise the system for the true ET event. A portion of Pro52 is present at the surface of amicyanin in close proximity to βV127 of MADH. In addition to the loss of three carbons of Pro52, the other consequence of the P52G mutation was a change in the position of the side chain of Met51, which prevented it from making close contacts with the side chain of βVal58 of MADH that are seen in the structure of the complex of native amicyanin with MADH (*28*).

The crystal structure of M51A amicyanin confirms the loss of three atoms of the Met51 side chain that contributes to hydrophobic interaction with the side chain of βVal58 of

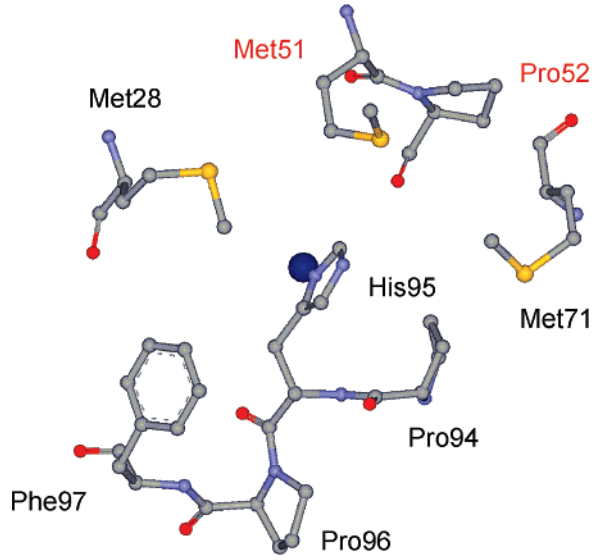

FIGURE 5: Hydrophobic residues of amicyanin that interact with MADH. The hydrophobic residues that surround the surface-exposed His95 which provides a ligand for copper (blue sphere) are shown.

MADH within the protein complex (Figure 6). It is noteworthy that while the P52G mutation caused about a 10-fold increase in the K_d for complex formation, the K_d for M51A is similar to that of native amicyanin. This means that the increase in K_d seen with the P52G mutation may be attributed to the specific change of residue 52 and not the accompanying change in the position of Met51. In contrast to this, the observed k_{ET} and values of λ and H_{AB} that describe the reaction of M51A amicyanin with *O*-quinol MADH are very similar to the reaction of P52G amicyanin and much different from that of native amicyanin (Table 3). This means that the decrease in k_3 and changes in ET parameters that were seen with the P52G mutation may be attributed to the change in position of the side chain of Met51 and not the loss of interactions involving Pro52.

Correct interpretation of the basis of the change in a rate constant and experimentally determined parameters for an ET reaction that results from site-directed mutagenesis depends on whether the observed reaction is true, gated, or coupled ET (*1*, *2*, *4*, *5*). We have previously shown that under physiological conditions, the reaction of *O*-quinol MADH to amicyanin is a true ET reaction (*17*, *18*), whereas the ET reaction from *N*-quinol MADH to amicyanin is chemically gated (*22*). The rate of the *N*-quinol reaction is that of the deprotonation of the *N*-quinol amino group, which is dependent on the presence of a monovalent cation (*20*, *23*). The rate of this reaction is actually much greater than that of the *O*-quinol reaction because the deprotonation results in a highly reactive, activated intermediate, which is optimized for ET (*23*).

The results of the thermodynamic analysis of ET indicate that the M51A amicyanin mutation converted the true ET reaction from *O*-quinol MADH into a conformationally gated ET reaction. Furthermore, this mutation decreased the rate of the reaction with *N*-quinol MADH to a value similar to that for the reaction with *O*-quinol MADH. This indicates that the same reaction step that gates the true ET reaction from *O*-quinol MADH also gates the otherwise rate-limiting proton-transfer reaction during the ET reaction from *N*-quinol MADH (Scheme 1). This is similar to what was observed previously as a consequence of the P52G mutation of amicyanin (*28*). For the M51A and P52G mutations to each convert a true ET reaction to one which is gated, each mutation must either introduce a new relatively slow reaction step that precedes ET, which is needed to optimize the system for the ET reaction, or cause a decrease in the rate of a relatively rapid pre-existing non-ET reaction step that is needed to optimize the system for the ET reaction. Since the P52G mutation also significantly altered the K_d value for the complex, that suggested that the protein−protein interface had been perturbed and thus supported the notion that for P52G amicyanin a conformational rearrangement would be required to switch from a redox-inactive stable complex (that with the larger K_d) to a redox-active but unstable complex ($[A_{ox}\text{-}B_{red}]^*$ in Scheme 1) (*28*). For M51A amicyanin, however, the K_d for complex formation is similar to native amicyanin, yet the values for λ and H_{AB} are very similar to that of P52G amicyanin. It is not obvious how the M51A mutation could introduce a new reaction step as was suggested for the P52G mutation since the binding process seems not to be perturbed. Therefore, it is likely that this mutation has slowed the rate of an existing but previously unrecognized conformational rearrangement that normally occurs in the native amicyanin−MADH complex subsequent to binding and prior to ET.

The results of the M51K and M51L mutations indicate that these also have consequences on the kinetic mechanism of regulation of the interprotein ET (Scheme 1). Their effects are intermediate between what is observed for the reactions of native amicyanin and M51A amicyanins (Figures 3 and 4). The ET parameters and the rate for the reaction of M51K amicyanin with *O*-quinol MADH are very similar to those for the reaction with M51A amicyanin. However, k_3 is greater than that for M51A amicyanin and less than that observed with native amicyanin. The salt dependence of the rate of the reaction of M51K amicyanin with *N*-quinol MADH plateaus at approximately the same salt concentration as that of the reaction of M51A but exhibits a greater rate. An explanation for these results is that the kinetic mechanism of interprotein ET is the same for M51K amicyanin as it is for M51A amicyanin, but that the value of k_x (k_{obs} for the gated reaction) for this mutant protein is greater than that for M51A amicyanin. In other words, the presence of a Lys as residue 52 slows the conformational rearrangement relative to Met but not to as great a degree as does Ala. The ET parameters and rate for the reaction of M51L with *O*-quinol MADH are very similar to the reaction with native amicyanin, and the salt dependence of the rate of the reaction with *N*-quinol MADH is somewhat intermediate between that of native and M51A amicyanins. Clearly, this conservative mutation has had the smallest effect on ET. The effect of this mutation on the conformational rearrangement denoted by k_x seems to be intermediary between those of the native complex with *N*-quinol MADH and the M51A complex with MADH. These relative profiles for the salt dependence of the rate with *N*-quinol MADH and the similarities in ET rate and parameters of the reactions of M51L amicyanin and native amicyanin with *O*-quinol MADH suggest for M51L amicyanin either that the values of k_x and k_3 are in the same range or that perhaps the equilibrium constant for the conformational change K_x is less favorable so that the

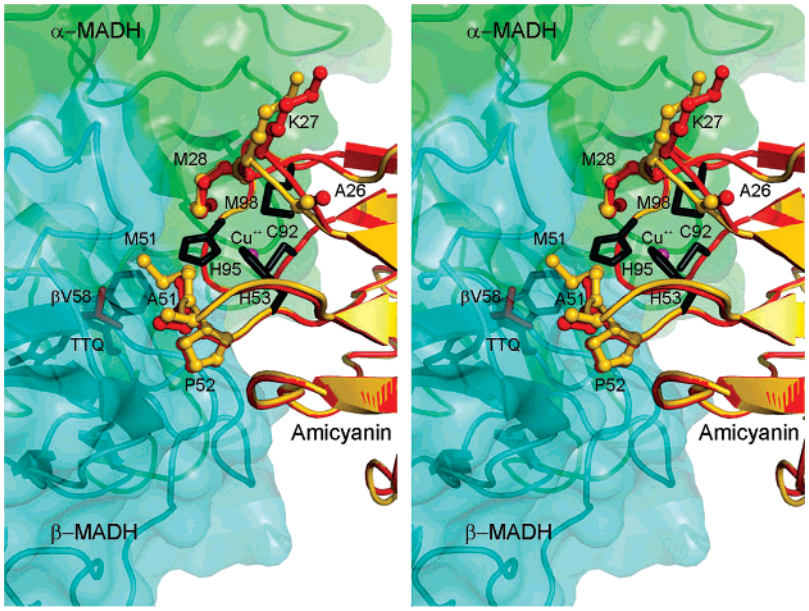

FIGURE 6: Changes in structure and position of residues that are located at the MADH−amicyanin interface in the complex caused by the M51A amicyanin (PDB ID 2QDV) mutation with respect to native amicyanin (PDB ID 2OV0). It should be noted that this is not a crystal structure of the complex of MADH with M51A amicyanin. For the purpose of illustration, the superimposed amicyanin structures are shown in relation to the MADH structure after alignment with the amicyanin portion of the MADH/amicyanin binary complex (PDB ID 2GC4). The two amicyanin structures are shown as ribbon cartoons with M51A red, native gold, and the affected residues of each as ball and stick with the same color code. The copper ion and the four coordinating side chains of M51A are shown as ball (purple) and stick (black), respectively. The MADH α-subunit (green) and β-subunit (cyan) are shown as ribbon cartoons and as partially transparent molecular surfaces with the TTQ side chains drawn as black sticks.

Scheme 1

$$A_{ox}+B_{red} \underset{}{\overset{K_d}{\rightleftharpoons}} A_{ox}\text{-}B_{red} \underset{k_{-X}}{\overset{k_X}{\rightleftharpoons}} [A_{ox}\text{-}B_{red}]^* \underset{k_{-ET}}{\overset{k_{ET}}{\rightleftharpoons}} A_{red}\text{-}B_{ox}$$

Kinetic mechanism of electron transfer from O-quinol MADH

$$A_{ox}+B_{red} \underset{}{\overset{K_d}{\rightleftharpoons}} A_{ox}\text{-}B_{red} \underset{k_{-X}}{\overset{k_X}{\rightleftharpoons}} [A_{ox}\text{-}B_{red}]^* \underset{k_{-PT}}{\overset{k_{PT}}{\rightleftharpoons}} [A_{ox}\text{-}B_{red}]^{**} \underset{k_{-ET}\bullet\bullet}{\overset{k_{ET}\bullet\bullet}{\rightleftharpoons}} A_{red}\text{-}B_{ox}$$

Kinetic mechanism of electron transfer from N-quinol MADH

Native amicyanin	$k_x >> k_{ET}$
P52G amicyanin	$k_x << k_{ET}$
M51A amicyanin	$k_x << k_{ET}$
M51K amicyanin	$k_x < k_{ET}$
M51L amicyanin	$k_x \sim k_{ET}$, or $K_x<1$

attenuation of rate could be attributed to a conversion to a kinetically coupled mechanism (*5*) where $k_{obs} = K_x \times k_{ET}$.

Another surprising and interesting observation is that the M51A mutation more so than the P52G mutation alters the position of residues 26−28 including Met28, which is also at the interface with MADH. While the ET parameters for the reaction of M51A amicyanin are much more similar to that of P52G amicyanin than to that of native amicyanin, there are some differences (Table 1). The k_3 for the reaction with M51A amicyanin is less than half that of the rate of P52G amicyanin, and the experimentally determined λ is 0.2 eV larger. Thus, it is possible that the perturbation of the position of Met28 is also affecting the rate and energy barrier of the conformational rearrangement (k_x in Scheme 1).

Summary. The strong similarity in the ET parameters and salt dependence of the rates for the reactions of P52G and M51A amicyanins with MADH strongly suggests that the reaction step that gates the ET reaction to M51A amicyanin is the same as that which gates the ET reaction to P52G amicyanin. In P52G amicyanin, close contacts are lost involving the three carbons of Pro52, the loss of which does not occur in the M51A mutant. The critical common feature of these two mutant amicyanins is that the interactions of the Met51 side chain with MADH are lost. The data presented here indicate that the loss of the interactions involving residue Pro52 is primarily responsible for the change in K_d for complex formation. The interactions involving the Met51 side chain are entirely responsible for the change in ET parameters and conversion of the true ET reaction of native amicyanin into the conformationally gated ET reaction. Since the K_d for complex formation is not affected by the M51A mutation, it follows that the change in the kinetic mechanism of the reaction is to reduce the rate of a pre-existing normally rapid conformational rearrangement rather than to introduce a new slow reaction step.

For soluble redox proteins to perform their physiological role, it is critical that they be able to recognize and specifically interact with their redox partners. Misdirected ET will result not only in the loss of energy for the cell but also the generation of reactive oxygen species or free radicals that will damage cellular components. We had previously shown that the stability of the amicyanin−MADH complex depended upon a unique combination of hydrophobic and electrostatic interactions between residues from each protein (*27*, *30*, *44*). We show here that subtle perturbations of these protein−protein interactions also have significant effects on the rates of ET with the protein complex. In fact, subtle changes in the identity of one specific amino acid residue, in this case Met51, is sufficient to dictate the mechanism and consequently the rate of a physiologic interprotein ET reaction. These results show that surface residues of redox

proteins may not only dictate specificity for their redox protein partners but also be critical to optimize the orientations of the redox centers and intervening media within the protein complex for the ET event.

REFERENCES

1. Davidson, V. L. (1996) Unraveling the kinetic complexity of interprotein electron transfer reactions, *Biochemistry 35*, 14035−14039.
2. Davidson, V. L. (2000) What controls the rates of interprotein electron-transfer reactions, *Acc. Chem. Res. 33*, 87−93.
3. Hoffman, B. M., and Ratner, M. A. (1987) Gated electron transfer: when are observed rates controlled by conformational interconversion? *J. Am. Chem. Soc. 109*, 6237−6243.
4. Davidson, V. L. (2002) Chemically gated electron transfer. A means of accelerating and regulating rates of biological electron transfer, *Biochemistry 41*, 14633−14636.
5. Davidson, V. L. (2000) Effects of kinetic coupling on experimentally determined electron transfer parameters, *Biochemistry 39*, 4924−4928.
6. Harris, T. K., Davidson, V. L., Chen, L., Mathews, F. S., and Xia, Z. X. (1994) Ionic strength dependence of the reaction between methanol dehydrogenase and cytochrome c-551i: evidence of conformationally coupled electron transfer, *Biochemistry 33*, 12600−12608.
7. Brunschwig, B. S., and Sutin, N. (1989) Directional electron transfer: Conformational interconversions and their effects on observed electron-transfer rate constants, *J. Am. Chem. Soc. 111*, 7454−7465.
8. Davidson, V. L. (2001) Pyrroloquinoline quinone (PQQ) from methanol dehydrogenase and tryptophan tryptophylquinone (TTQ) from methylamine dehydrogenase, *Adv. Protein Chem. 58*, 95−140.
9. Husain, M., and Davidson, V. L. (1985) An inducible periplasmic blue copper protein from *Paracoccus denitrificans*. Purification, properties, and physiological role, *J. Biol. Chem. 260*, 14626−14629.
10. Husain, M., and Davidson, V. L. (1986) Characterization of two inducible periplasmic *c*-type cytochromes from *Paracoccus denitrificans*, *J. Biol. Chem. 261*, 8577−8580.
11. Chen, L., Durley, R., Poliks, B. J., Hamada, K., Chen, Z., Mathews, F. S., Davidson, V. L., Satow, Y., Huizinga, E., and Vellieux, F. M. (1992) Crystal structure of an electron-transfer complex between methylamine dehydrogenase and amicyanin, *Biochemistry 31*, 4959−4964.
12. Chen, L., Durley, R. C., Mathews, F. S., and Davidson, V. L. (1994) Structure of an electron transfer complex: methylamine dehydrogenase, amicyanin, and cytochrome *c*551i, *Science 264*, 86−90.
13. Merli, A., Brodersen, D. E., Morini, B., Chen, Z., Durley, R. C., Mathews, F. S., Davidson, V. L., and Rossi, G. L. (1996) Enzymatic and electron transfer activities in crystalline protein complexes, *J. Biol. Chem. 271*, 9177−9180.
14. Ferrari, D., Di Valentin, M., Carbonera, D., Merli, A., Chen, Z.-W., Mathews, F. S., Davidson, V. L., and Rossi, G.-L. (2004) Electron transfer in crystals of the binary and ternary complexes of methylamine dehydrogenase with amicyanin and cytochrome *c*551i as detected by EPR spectroscopy, *J. Biol. Inorg. Chem 9*, 231−237.
15. McIntire, W. S., Wemmer, D. E., Chistoserdov, A., and Lidstrom, M. E. (1991) A new cofactor in a prokaryotic enzyme: tryptophan tryptophylquinone as the redox prosthetic group in methylamine dehydrogenase, *Science 252*, 817−824.
16. Davidson, V. L., and Jones, L. H. (1991) Intermolecular electron transfer from quinoproteins and its relevance to biosensor technology, *Anal. Chim. Acta 249*, 235−240.
17. Brooks, H. B., and Davidson, V. L. (1994) Kinetic and thermodynamic analysis of a physiologic intermolecular electron-transfer reaction between methylamine dehydrogenase and amicyanin, *Biochemistry 33*, 5696−5701.
18. Brooks, H. B., and Davidson, V. L. (1994) Free energy dependence of the electron transfer reaction between methylamine dehydrogenase and amicyanin, *J. Am. Chem. Soc. 116*, 11201−11202.
19. Bishop, G. R., and Davidson, V. L. (1998) Electron transfer from the aminosemiquinone reaction intermediate of methylamine dehydrogenase to amicyanin, *Biochemistry 37*, 11026−11032.
20. Bishop, G. R., and Davidson, V. L. (1995) Intermolecular electron transfer from substrate-reduced methylamine dehydrogenase to amicyanin is linked to proton transfer, *Biochemistry 34*, 12082−12086.
21. Davidson, V. L., Brooks, H. B., Graichen, M. E., Jones, L. H., and Hyun, Y. L. (1995) Detection of intermediates in tryptophan tryptophylquinone enzymes, *Methods Enzymol. 258*, 176−190.
22. Davidson, V. L., and Sun, D. (2003) Evidence for substrate activation of electron transfer from methylamine dehydrogenase to amicyanin, *J. Am. Chem. Soc. 125*, 3224−3225.
23. Bishop, G. R., and Davidson, V. L. (1997) Catalytic role of monovalent cations in the mechanism of proton transfer which gates an interprotein electron transfer reaction, *Biochemistry 36*, 13586−13592.
24. Cunane, L. M., Chen, Z., Durley, R. C. E., and Mathews, F. S. (1996) X-ray crystal structure of the cupredoxin amicyanin from *Paracoccus denitrificans*, refined at 1.31 Å resolution, *Acta Crystallogr., Sect. D 52*, 676−686.
25. Carrell, C. J., Sun, D., Jiang, S., Davidson, V. L., and Mathews, F. S. (2004) Structural studies of two mutants of amicyanin from *Paracoccus denitrificans* that stabilize the reduced state of the copper, *Biochemistry 43*, 9372−9380.
26. Sun, D., and Davidson, V. L. (2003) Effects of engineering uphill electron transfer into the methylamine dehydrogenase-amicyanin-cytochrome *c*-551i complex, *Biochemistry 42*, 1772−1776.
27. Davidson, V. L., Jones, L. H., and Zhu, Z. (1998) Site-directed mutagenesis of Phe 97 to Glu in amicyanin alters the electronic coupling for interprotein electron transfer from quinol methylamine dehydrogenase, *Biochemistry 37*, 7371−7377.
28. Ma, J. K., Carrell, C. J., Mathews, F. S., and Davidson, V. L. (2006) Site-directed mutagenesis of proline 52 to glycine in amicyanin converts a true electron transfer reaction into one that is conformationally gated, *Biochemistry 45*, 8284−8293.
29. Davidson, V. L. (1990) Methylamine dehydrogenases from methylotrophic bacteria, *Methods Enzymol. 188*, 241−246.
30. Davidson, V. L., Jones, L. H., Graichen, M. E., Mathews, F. S., and Hosler, J. P. (1997) Factors which stabilize the methylamine dehydrogenase-amicyanin electron transfer protein complex revealed by site-directed mutagenesis, *Biochemistry 36*, 12733−12738.
31. Chistoserdov, A. Y., Boyd, J., Mathews, F. S., and Lidstrom, M. E. (1992) The genetic organization of the *mau* gene cluster of the facultative autotroph *Paracoccus denitrificans*, *Biochem. Biophys. Res. Commun. 184*, 1181−1189.
32. Zhu, Z., Cunane, L. M., Chen, Z., Durley, R. C., Mathews, F. S., and Davidson, V. L. (1998) Molecular basis for interprotein complex-dependent effects on the redox properties of amicyanin, *Biochemistry 37*, 17128−17136.
33. Cammack, R. (1995) in *Bioenergetics: A Practical Approach* (Brown, G. C., and Cooper, C. E., Eds.) pp 85−109, IRL Press, New York.
34. Ma, J. K., Bishop, G. R., and Davidson, V. L. (2005) Role of the Type I copper center in determining the stability of amicyanin, *Arch. Biochem. Biophys. 444*, 27−33.
35. Bishop, G. R., Brooks, H. B., and Davidson, V. L. (1996) Evidence for a tryptophan tryptophylquinone aminosemiquinone intermediate in the physiologic reaction between methylamine dehydrogenase and amicyanin, *Biochemistry 35*, 8948−8954.
36. Marcus, R. A., and Sutin, N. (1985) Electron transfers in chemistry and biology, *Biochim. Biophys. Acta 811*, 265−322.
37. Lim, L. W., Mathews, F. S., Husain, M., and Davidson, V. L. (1986) Preliminary X-ray crystallographic study of amicyanin from *Paracoccus denitrificans*, *J. Mol. Biol. 189*, 257−258.
38. Otwinowski, Z., and Minor, W. (1997) Processing of x-ray diffraction data collected by oscillation methods, *Methods Enzymol. 276*, 307−326.
39. Sheldrick, G. M., and Schneider, T. R. (1997) SHELXL: high resolution refinement, *Methods Enzymol. 277*, 319−343.
40. Kleywegt, G. J., and Jones, T. A. (1995) Where freedom is given, liberties are taken, *Structure 3*, 535−540.
41. Winkler, J. R., and Gray, H. B. (1992) Electron transfer in ruthenium-modified proteins, *Chem. Rev. 92*, 369−379.
42. Morris, A. L., MacArthur, M. W., Hutchinson, E. G., and Thornton, J. M. (1992) Stereochemical quality of protein structure coordinates, *Proteins 12*, 345−364.
43. Carrell, C. J., Ma, J. K., Antholine, W. E., Hosler, J. P., Mathews, F. S., and Davidson, V. L. (2007) Generation of novel copper

sites by mutation of the axial ligand of amicyanin. Atomic resolution structures and spectroscopic properties, *Biochemistry 46*, 1900−1912.
44. Zhu, Z., Jones, L. H., Graichen, M. E., and Davidson, V. L. (2000) Molecular basis for complex formation between methylamine dehydrogenase and amicyanin revealed by inverse mutagenesis of an interprotein salt bridge, *Biochemistry 39*, 8830−8836.
45. Brünger, A. T. (1992) Free R-value: a novel statistical quantity for assessing the accuracy of crystal structures, *Nature 355*, 472−475.
46. Gray, H. B., and Winkler, J. R. (2005) Long-range electron transfer, *Proc. Natl. Acad. Sci. U.S.A. 102*, 3534−3539.

BI7012307